A&A 496, 45–50 (2009)
DOI: 10.1051/0004-6361:200810876

Astronomy & Astrophysics

New CO detections of lensed submillimetre galaxies in A2218: probing molecular gas in the LIRG regime at high redshift⋆,⋆⋆

K. K. Knudsen[1], R. Neri[2], J.-P. Kneib[3], and P. P. van der Werf[4]

[1] Argelander-Institut für Astronomie, Auf dem Hügel 71, 53123 Bonn, Germany
e-mail: knudsen@astro.uni-bonn.de
[2] Institut de Radio Astronomie Millimétrique (IRAM), 300 rue de la Piscine, Domaine Universitaire de Grenoble, St. Martin d'Hères 38406, France
[3] Laboratoire d'Astrophysique de Marseille, OAMP, Université Aix-Marseille & CNRS, 38 rue F. Joliot-Curie, 13388 Marseille Cedex 13, France
[4] Leiden Observatory, Leiden University, PO Box 9513, 2300 RA Leiden, The Netherlands

Received 28 August 2008 / Accepted 25 November 2008

ABSTRACT

Context. Submillimetre galaxies (SMGs) are distant, dusty galaxies undergoing star formation at prodigious rates. Recently there has been major progress in understanding the nature of the bright SMGs (i.e. $S_{850\,\mu m} > 5$ mJy). The samples for the fainter SMGs are small and are currently in a phase of being built up through identification studies.
Aims. We study the molecular gas content in the two SMGs, SMMJ163555 and SMMJ163541, at redshifts $z = 1.034$ and $z = 3.187$ with unlensed submillimetre fluxes of 0.4 mJy and 6.0 mJy. Both SMGs are gravitationally lensed by the foreground cluster Abell 2218.
Methods. We used the IRAM Plateau de Bure Interferometer to obtain observations at 3 mm of the lines CO(2–1) for SMMJ163555 and CO(3–2) for SMMJ163541. Additionally, we obtained CO(4–3) observations for the candidate $z = 4.048$ SMMJ163556 with an unlensed submillimetre flux of 2.7 mJy.
Results. The CO(2–1) line was detected for SMMJ163555 at redshift 1.0313 with an integrated line intensity of 1.2 ± 0.2 Jy km s^{-1} and a line width of 410 ± 120 km s^{-1}. From this a gas mass of $1.6 \times 10^9\,M_\odot$ is derived and a star formation efficiency of $440\,L_\odot/M_\odot$ estimated. The CO(3–2) line was detected for SMMJ163541 at redshift 3.1824, possibly with a second component at redshift 3.1883, with an integrated line intensity of 1.0 ± 0.1 Jy km s^{-1} and a line width of 280 ± 50 km s^{-1}. From this a gas mass of $2.2 \times 10^{10}\,M_\odot$ is derived and a star formation efficiency of $1000\,L_\odot/M_\odot$ is estimated. For SMMJ163556, the CO(4–3) is undetected within the redshift range 4.035−4.082 down to a sensitivity of 0.15 Jy km s^{-1}.
Conclusions. Our CO-line observations confirm the optical redshifts for SMMJ163555 and SMMJ163541. The CO-line luminosity $L'_{\rm CO}$ for both galaxies is consistent with the $L_{\rm FIR} - L'_{\rm CO}$ relation. SMMJ163555 has the lowest far-infrared luminosity of all SMGs with a known redshift and is one of the few high-redshift LIRGs whose properties can be estimated prior to ALMA.

Key words. galaxies: evolution – galaxies: high-redshift – galaxies: ISM – galaxies: starburst

1. Introduction

Observations of CO in high redshift galaxies are instrumental in assessing the quantity of the molecular gas available for star formation. The submillimetre galaxies (SMGs; see Blain et al. 2002, for review) are dusty galaxies undergoing star formation at prodigious rates, $>1000\,M_\odot\,{\rm yr}^{-1}$ with a redshift distribution peaking at $z \sim 2.5$ (Chapman et al. 2005). Previous CO results of SMGs have shown that SMGs can harbour molecular gas reservoirs of the order of $10^{10}\,M_\odot$, enabling the massive starburst to build stars during 10–100 Myr. It is thus likely that SMGs are the progenitors of the nearby massive ellipticals (e.g. Chapman et al. 2005; Greve et al. 2005; Lapi et al. 2006; Tacconi et al. 2006; Nesvadba et al. 2007).

Hitherto the CO results of SMGs have been obtained primarily for SMGs with intrinsic fluxes $S_{850\,\mu m} > 2$ mJy (Frayer et al. 1998, 1999; Neri et al. 2003; Genzel et al. 2003; Downes & Solomon 2003; Tacconi et al. 2006, 2008). Of the five known SMGs with lensing corrected $S_{850\,\mu m} < 1$ mJy (Kneib et al. 2004; Borys et al. 2004; Knudsen et al. 2006, 2008b), only the triply-imaged galaxy SMMJ16359+6612 has previously been detected in CO (Sheth et al. 2004; Kneib et al. 2005; Weiß et al. 2005). Through statistical studies, it is clear that other high-redshift galaxies populations, such distant red galaxies, extremely red objects, and BzK galaxies have an average 850 μm flux $\leq$1 mJy (e.g. Webb et al. 2004; Knudsen et al. 2005; Daddi et al. 2005), and thus there will be an overlap between these and the faint SMGs. However, none of them have individual detections at these low flux density levels due to the SCUBA 850 μm confusion limit, making it difficult to establish the exact link between the faint SMGs and other galaxy populations.

In this paper we report the IRAM Plateau de Bure Interferometer (PdBI) observations of two strongly lensed SMGs, both present in the galaxy cluster field Abell 2218 (Knudsen et al. 2006). SMM J163555.2+661150 (henceforth SMMJ163555) has an optical counterpart at redshift $z = 1.034$,

⋆ Based on observations obtained at the IRAM Plateau de Bure Interferometer (PdBI). IRAM is funded by the Centre National de la Recherche Scientifique (France), the Max-Planck Gesellschaft (Germany), and the Instituto Geografico Nacional (Spain).
⋆⋆ The three spectra cubes (FITS files corresponding to the maps of Fig. 2) are only available in electronic form at the CDS via anonymous ftp to cdsarc.u-strasbg.fr (130.79.128.5) or via http://cdsweb.u-strasbg.fr/cgi-bin/qcat?J/A+A/496/45

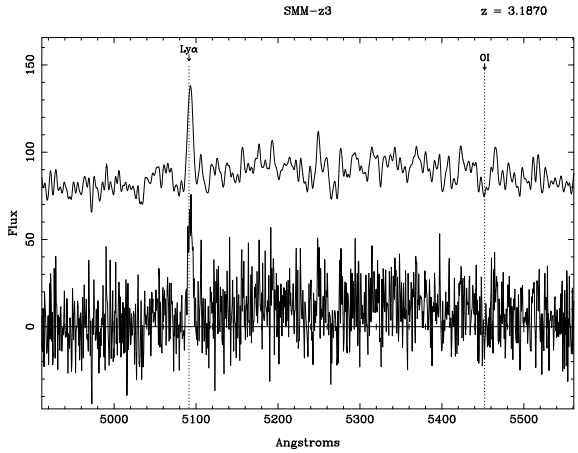

Fig. 1. The optical spectrum of SMMJ163541, where the dotted lines show the Lyα and OI features. On the bottom, we show the original spectrum and on the top the spectrum is smoothed using a $\sigma = 3$ pixel Gaussian and shifted in the vertical direction for clarity.

which is also known as Galaxy #289 in the notation of Pelló et al. (1992). It has an unlensed 850 μm flux of 0.4 mJy and is one of the lowest redshift SMGs (cf. SMM J02396-0134; Smail et al. 2002), making it the SMG with the lowest far-infrared luminosity known so far. SMM J163541.2+661144 (henceforth SMMJ163541) has been identified with a galaxy at redshift $z = 3.187$. The optical spectroscopy is also presented in this paper. With its unlensed 850 μm flux of 6.0 mJy it belongs to the bright SMGs as found typically in the blank field surveys. SMMJ163555.5+661300 (henceforth SMMJ163556) has an unlensed 850 μm flux of 2.7 mJy and has a candidate optical counterpart at redshift $z = 4.048$ (Knudsen et al. 2008a), possibly placing it among the highest redshift SMGs known.

Throughout the paper we assume a cosmology with $H_0 = 70\,\mathrm{km\,s^{-1}\,Mpc^{-1}}$, $\Omega_\mathrm{m} = 0.3$, and $\Omega_\Lambda = 0.7$.

2. Observations

2.1. Optical spectroscopy

On 2003 June 30 and July 1, we conducted deep multislit spectroscopy with a low-resolution imaging spectrograph (LRIS; Oke et al. 1995) at the 10 m W.M. Keck telescope at Mauna Kea, Hawaii, of sources lying in the field of the rich cluster A2218 (see Kneib et al. 2004). The two nights had reasonable seeing, ~0.8 arcsec, but were not fully photometric (with some cirrus); nevertheless, we obtained a crude flux calibration of our observations using Feige 67 and 110 as spectrophotometric standard stars. We observed SMM163541 for a total of 2.9 h using the 600/4000 blue grism and the 400/8500 red gratings offering a spectral dispersion of 0.63 Å pixel[1] in the blue and 1.8 Å pixel^{-1} in the red, respectively. The spectrum of SMM163541 shows a strong Lyα emission and a possible OI metal line (Fig. 1). The redshift derived is $z = 3.187 \pm 0.001$ based on Ly-alpha emission.

Optical spectroscopy for SMMJ163555 and SMMJ163556 have been presented elsewhere (Pelló et al. 1992; Knudsen et al. 2008a).

2.2. IRAM Plateau de Bure

Observations of SMMJ163555, SMMJ163541, and SMMJ163556 were carried out during May, June, July, August, and September 2005 with the IRAM PdBI consisting of six 15 m diameter antennas in the compact D configuration. The correlator was configured for the CO line and continuum observations to simultaneously cover 580 MHz in the 3 and 1.3 mm bands. In the case of SMMJ163556, the frequency setting was re-adjusted during the observations to add more observations to a tentative detection. Consequently, the sensitivity varies across the final spectrum. The total integration time was 15.9 h, 14.3 h, and 17.3 h for SMMJ163555, SMMJ163541, and SMMJ163556, respectively. All sources were observed in good observing conditions, where the typical system temperatures at 3 mm were 100–250 K. The data were reduced and analysed using the IRAM GILDAS software. Bright quasars were used for passband calibration. The phase and amplitude variations within each track were calibrated out by interleaving reference observations of the calibrator source 1637+574 every 20 min. The overall flux scale for each epoch was set on MWC 349. Finally, naturally weighted data cubes were created, and the final beam in the maps at 3 mm were $6.8'' \times 4.9''$, $9.8'' \times 7.2''$, and $7.4'' \times 5.9''$ for SMMJ163555, SMMJ163541, and SMMJ163556, respectively.

3. Results

Figure 2 shows the CO spectra and maps, and the resulting observational results are listed in Table 1. Additionally, the CO contours have been overlayed on an optical image in Fig. 3. The CO(2–1) line for SMMJ163555 and the CO(3–2) line for SMMJ163541 were successfully detected. To obtain the fux, the line width, and the corresponding uncertainties, which are given in Table 1, we fit a single Gaussian to the lines. The uncertainty of the integrated line intensity, I_CO, is obtained from the fitting of a single point source to the map. The line intensity is obtained from the Gaussian fit and is in good agreement with the integral determined from the single point source fitting. We note that both lines are offset by –330 km s^{-1} and –400 km s^{-1} (bluewards) from the UV (SMMJ163541) and optical (SMMJ163555) spectroscopic redshifts, respectively. SMMJ163541 appears to have a second fainter CO component with a redshift of $z = 3.1883$, and while deeper observations are required to confirm this, we note that double-peak CO profiles appear to be common for SMGs (Greve et al. 2005). The discrepancy between the optical and CO redshifts could be in either case be due to a blend of two sources, in particular as we see in the case of SMMJ163541. There is no clear evidence of an AGN that could drive an outflow.

CO(4–3) was undetected for SMMJ163556. A 2.8σ continuum signal is found at the position 16:35:56.01, +66:12:54.3. As this is 5″ away from the phase tracking centre, we attribute this to noise; also no source was found at this position at other wavelengths.

The 3.0 mm continuum emission was not detected for either source and we place 3σ upper limits. That none of the sources were detected in the continuum at 3 mm agrees with the observed 850 μm fluxes (Knudsen et al. 2006). As the observations were carried out during the summer months, the conditions were not useful for 1.3 mm observations, and neither line nor continuum was detected.

4. Discussion

4.1. Luminosities

We derive the CO line luminosities from the velocity-integrated line flux density following Solomon et al. (1997). We

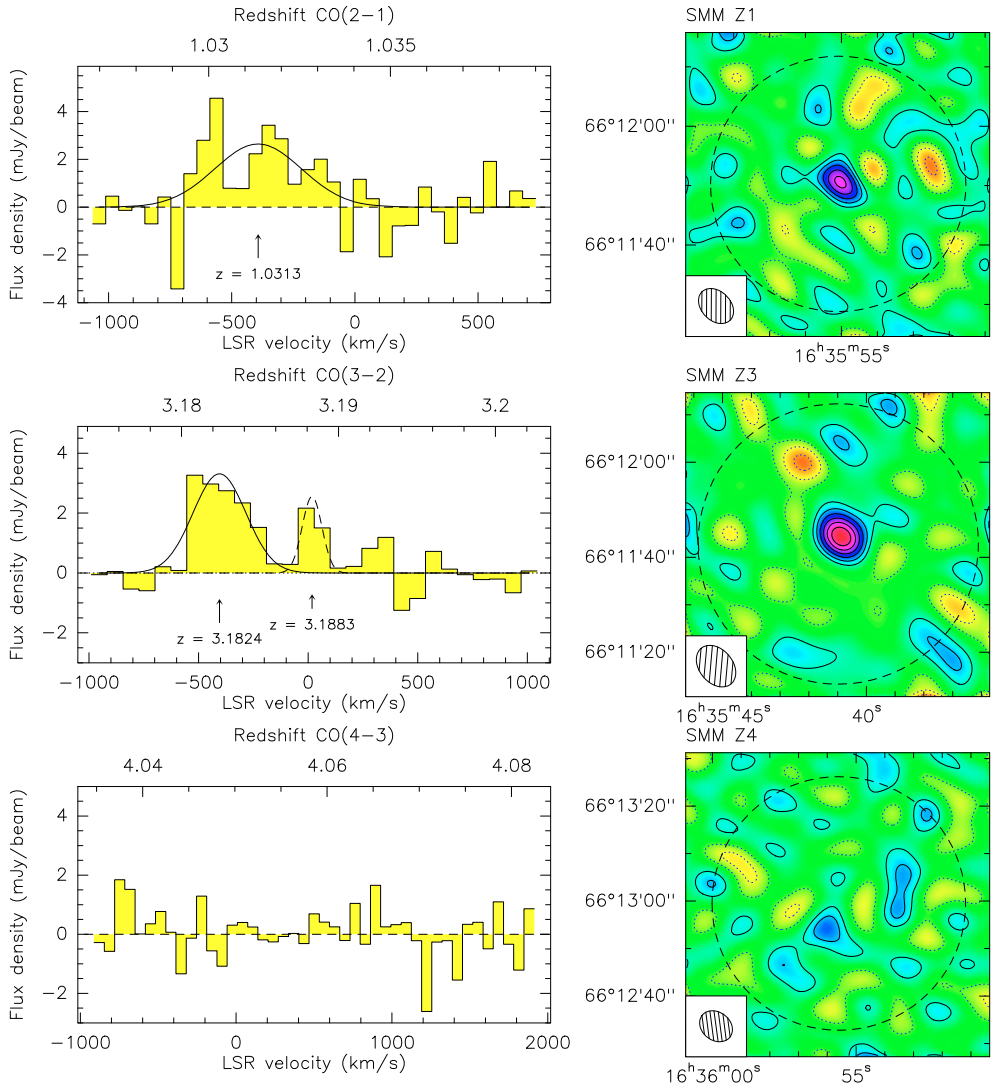

Fig. 2. The resulting spectra and maps from the IRAM CO observations. *Top panel*: the CO(2 → 1) detection of SMMJ163555 (z = 1.0313). *Middle panel*: the CO(3 → 2) detection of SMMJ163541 (z = 3.1824). *Bottom panel*: the extracted spectrum at the position of SMMJ163556. The velocity intervals used for producing the maps on the right side are: SMMJ163555: –695 to –75 km s^{-1}, SMMJ163541: –265 to –555 km s^{-1}, and SMMJ163556: the whole velocity range. The contours in the maps are in steps of 1σ, where the solid and dashed lines indicate positive and negative values, respectively. The large dashed circle indicates the primary beam.

Table 1. Observational results for SMMJ163555, SMMJ163541, SMMJ163556.

Source	Transition	z_{CO}	RA (J2000.0)	Dec (J2000.0)	σ_{pos} $^{\circ}$ [″]	I_{CO} [Jy km s^{-1}]	Flux† [mJy]	Line width [km s^{-1}]
SMMJ163555	CO(2–1)	1.0313 ± 0.0012	16 35 55.05	+66 11 50.7	∼0.5	1.2 ± 0.2	2.6 ± 0.7	410 ± 120
	3 mm						<1.4	
SMMJ163541	CO(3–2)	3.1824 ± 0.0017	16 35 40.86	+66 11 44.4	∼0.4	1.0 ± 0.1	3.3 ± 0.4	284 ± 50
	CO(3–2)	3.1883 ± 0.0006	16 35 41.33	+66 11 46.4	∼0.8	0.3 ± 0.1	2.6 ± 0.7	106 ± 44
	3 mm						<0.6	
SMMJ163556	CO(4–3)	4.035–4.082‡				<0.45*		
	3 mm						<0.44	

† For line emission this refers to the peak flux, for continuum this refers to the flux density; ‡ the corresponding redshift ranged in which the CO(4–3) transition would have been detectable; * 3σ upper limit estimated assuming a line width of 400 km s^{-1}. $^{\circ}$ σ_{pos} refers to the uncertainty on the position.

estimate the far-infrared luminosity by assuming a modified blackbody spectral energy distribution (SED) with a temperature of T = 35 K and β = 1.5; SMMJ163555 has a 450 μm detection of 17.1 mJy (Knudsen et al. 2008b), so the Rayleigh-Jeans tail is well-matched to this. SMM163541 is detected in the 450 μm map; however, it is very close to the noisy edge of the map, so the determined flux of 53 ± 16 mJy might be overestimated, by possibly up to 50%, making it consistent with a temperature of 35 K. For SMMJ163555, L_{FIR} is in good agreement with the ISOCAM result from Biviano et al. (2004). The unlensed luminosities are

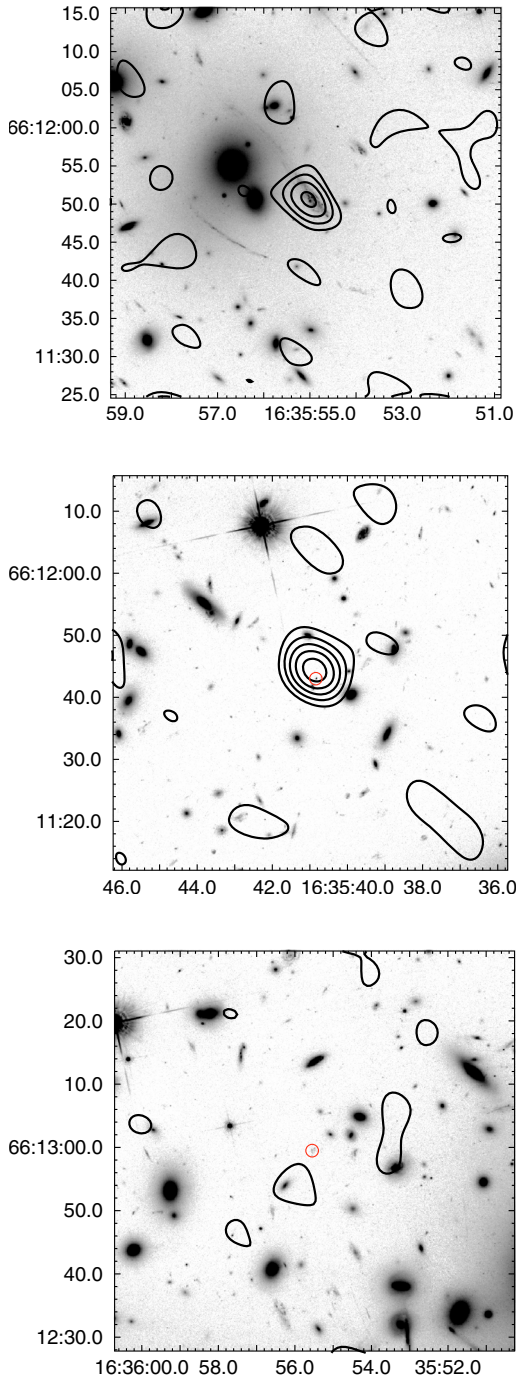

Fig. 3. The CO contours overlayed on the ACS F775W image. *Top*: SMMJ163555 with the contour levels 0.0005, 0.001, ... Jy/beam; *middle*: SMMJ163541 with same contour levels, the red circle shows the optical position; *bottom*: SMMJ163556 with the contour level 0.00025 Jy/beam, the red circle shows the optical position.

given in Table 2. The gravitational lensing magnification is determined using LENSTOOL (Kneib et al. 1993) with the detailed mass model of A2218 (Elíasdóttir et al. 2008) as input. It should be noted that the far-infrared luminosities of SMGs are often based on only one or two submillimetre flux density data points and an assumed SED; hence, until more far-infrared wavelengths observations have been obtained for SMGs, their far-infrared luminosities will be uncertain.

It has been known for many years that a relation exists between the far-infrared luminosity and the CO luminosity of star-forming galaxies (e.g. Young et al. 1986; Solomon et al. 1997). This relation appears to be valid over a wide range of luminosities, ranging from disc galaxies to high-redshift QSOs. In Fig. 4, we compare the CO results with those from previous works and find that both SMMJ163555 and SMMJ163541 exhibit similar behaviour. The 3σ $L'_{\rm CO}$ upper limit for SMMJ163556 is below the $L_{\rm FIR}/L'_{\rm CO}$ relation, indicating that the CO line might be outside of the redshift range probed by our observations. We notice that the ratio $L_{\rm FIR}/L'_{\rm CO}$ of 350 for SMMJ163555 is similar to that of SMMJ16359+6612 (Sheth et al. 2004; Kneib et al. 2005). These are both faint SMGs with unlensed submillimetre fluxes below the blank field confusion limit of SCUBA at 850 μm and have far-infrared luminosities comparable to that of the local ULIRGs (e.g. Solomon et al. 1997); however, their $L_{\rm FIR}/L'_{\rm CO}$ ratio is higher than most of the ULIRGs in the Solomon et al. (1997) sample. A CO detection for other such faint SMGs is needed to conclude whether this is a trend or just a consequence of the scatter.

We performed a straight-line least squares fit to the far-infrared luminosity and the CO line luminosity of SMMJ163541, SMMJ163555, and the known high-redshift SMGs and QSOs (Frayer et al. 1998, 1999; Neri et al. 2003; Genzel et al. 2003; Downes & Solomon 2003; Sheth et al. 2004; Kneib et al. 2005; Greve et al. 2005; Tacconi et al. 2006; Barvainis et al. 1994; Omont et al. 1996; Guilloteau et al. 1997; Downes et al. 1999; Planesas et al. 1999; Guilloteau et al. 1999; Cox et al. 2002; Barvainis et al. 2002; Walter et al. 2003; Hainline et al. 2004; Riechers et al. 2006; Coppin et al. 2008), treating both $L_{\rm FIR}$ and $L'_{\rm CO}$ as independent variables with uncorrelated errors and ignoring the upper limits. For the combined SMGs and QSO sample, we find $\log L_{\rm FIR} = (1.16 \pm 0.05) \log L'_{\rm CO} + 1.03$, for the SMG sample $\log L_{\rm FIR} = (1.33 \pm 0.07) \log L'_{\rm CO} - 0.69$, and for the QSO sample $\log L_{\rm FIR} = (1.07 \pm 0.06) \log L'_{\rm CO} + 1.92$. Similar results were obtained when excluding SMMJ163555. When including the four other high-redshift CO detections of LBG and BzK galaxies (Baker et al. 2004; Coppin et al. 2007; Daddi et al. 2008) to the combined SMGs and QSO sample, we find a consistent result: $\log L_{\rm FIR} = (1.26 \pm 0.04) \log L'_{\rm CO} - 0.02$. In the luminosity range $L_{\rm FIR} = 10^{11}-10^{14}$, the resulting three fits are virtually identical, and the deviation from previous fits that combine high and low redshifts samples (Greve et al. 2005; Riechers et al. 2006) is no more than 1σ.

With the CO detection of SMMJ163555 we can now probe the high-redshift luminous IR galaxy (LIRG) regime, which will otherwise only be accessible with future instruments such as ALMA. For the CO line luminosity of SMMJ163555 of 2×10^9 K km s^{-1} pc^{-2} the predictions for $L_{\rm FIR}$, hence the star formation rate (SFR), are a factor 3–5 higher for the high-redshift galaxies compared to that of the nearby galaxies, using the fits from above. Given the rather sparse statistics for the high-redshift galaxies in the LIRG regime, we cannot draw conclusions, but we can speculate that the high-redshift galaxies might have a higher $L_{\rm FIR}$-to-$L'_{\rm CO}$ ratio, which can be used as a proxy for star formation efficiency, than the nearby ones. Bouché et al. (2007) also find in their comparison of the star formation properties of various $z \sim 2$ star-forming galaxy populations that these have higher star formation efficiency.

4.2. H_2 gas mass

Assuming that the CO is thermalised to at least the $J = 3 \rightarrow 2$ transition, we can convert the CO line luminosity into a

Table 2. Derived properties for SMMJ163555 and SMMJ163541.

	D_A [Gpc]	μ^a	$D = 1''$ [kpc]	L'_{CO} [K km s^{-1} pc^2]	M_{gas} [$M_\odot$]	L_{FIR} [$L_\odot$]
SMMJ163555	1.66	7.1	1.1	2.3×10^9	1.8×10^9	4.5×10^{11}
SMMJ163541	1.57	1.7	4.4	2.8×10^{10}	2.2×10^{10}	1.5×10^{13}
– two comp.				3.6×10^{10}	2.9×10^{10}	
SMMJ163556	1.42	4.2	1.6	$<0.4 \times 10^{10b}$	$<0.3 \times 10^{10}$	8.0×10^{12}

[a] Gravitational lensing magnification; [b] based on the upper limit from Table 1 assuming a line width of 400 km s^{-1}.

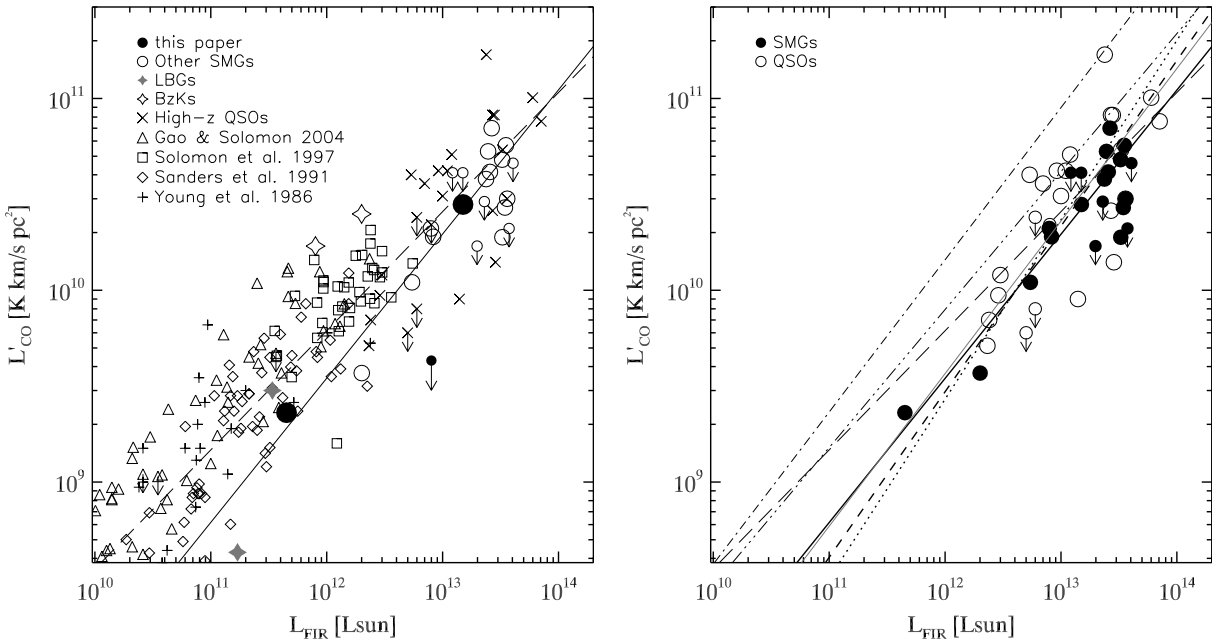

Fig. 4. *Left panel*: the CO luminosity plotted versus the far-infrared luminosity for SMMJ163555 and SMMJ163541. For comparison the results for other submillimetre galaxies are plotted (Frayer et al. 1998, 1999; Neri et al. 2003; Genzel et al. 2003; Downes & Solomon 2003; Sheth et al. 2004; Kneib et al. 2005; Greve et al. 2005; Tacconi et al. 2006) along with low-redshift and local ULIRG, LIRG, and starburst galaxy results (Young et al. 1986; Sanders et al. 1991; Solomon et al. 1997; Gao & Solomon 2004), high-redshift quasars (Barvainis et al. 1994; Omont et al. 1996; Guilloteau et al. 1997; Downes et al. 1999; Planesas et al. 1999; Guilloteau et al. 1999; Cox et al. 2002; Barvainis et al. 2002; Walter et al. 2003; Hainline et al. 2004; Riechers et al. 2006; Coppin et al. 2008) and LBG and BzK galaxies (Baker et al. 2004; Coppin et al. 2007; Daddi et al. 2008). The solid line is the least-square fit to the SMG sample and the long-dashed line shows the best-fit line to the log L_{FIR} − log L'_{CO} from Greve et al. (2005) for SMGs combined with low-redshift (U)LIRGs. *Right panel*: same as above, though only plotting the high-redshift SMGs and QSOs. The solid line is the least-square fit to the SMG sample, the dotted line the fit to the QSO sample, the dashed line the fit to the combined high-z sample, and the grey solid line is the fit to the combined SMGs, QSOs, LBGs, and BzKs sample. The thin lines are from the previous fit to combined high and low-redshift samples, long-dashed from Greve et al. (2005) and the dash-dot and dash-dot-dot-dot are from Riechers et al. (2006), where the former is the fit to the Gao & Solomon sample and the latter is the fit to the combined high redshift sources, the Gao & Solomon sample, Solomon et al. (1997) sample, and PG QSOs samples.

molecular gas mass. We use a factor of $\alpha_{CO} = M_{H_2}/L'_{CO(1-2)} = 0.8\ M_\odot/(\mathrm{K\,km\,s^{-1}\,pc^2}) = 0.2\alpha_{CO}$(Galactic), as derived from observations of $z \sim 0.1$ ULIRGs (Downes & Solomon 1998). The gas masses are probably uncertain by a factor of at least 2. For SMMJ163555, which is in the LIRG regime, the conversion factor may well be closer to that for normal galaxies, hence the H_2 mass can be correspondly higher. The results, which have been corrected for gravitational lensing, are shown in Table 2. The line widths of SMMJ163555 and SMMJ163541 are 410 and 284 km s^{-1}, respectively, which is about half of the median value of 780 km s^{-1} from the large sample studied by Greve et al. (2005), but comparable to the values for the SMMJ16359+6612 (Kneib et al. 2005).

The line profile can be used for deriving the line width, which we use for estimating a dynamical mass. This estimate has large uncertainties due to the moderate signal-to-noise ratio of the spectrum, and the lack of spatial information due to the large beam. Assuming a disc model, we use $M_{dyn} \sin^2 i\ (M_\odot) = 4.2 \times 10^4 \Delta v^2_{FWHM} R$ (see Neri et al. 2003) to estimate the dynamical mass. First we solve the empirical Schmidt-Kennicutt relation as deduced for high-redshift starburst galaxies $\Sigma_{sf}[M_\odot\,\mathrm{yr^{-1}\,kpc^{-2}}] = 9.3 \times 10^{-5}(\Sigma_{gas}[M_\odot\,\mathrm{pc^{-2}}])^{1.71}$ from Bouché et al. (2007) for the source size, deriving the gas surface density from $\sigma_{gas} = f_{gas} M_{dyn} R/(\pi R^2)$, assuming $f_{gas} = 0.4$ and the star formation rate surface density from $\Sigma_{sf} = SFR/(\pi R^2)$. Not knowing the inclination, i, we apply an average $\langle \sin(i) \rangle = \pi/4$, which means a correction of $\langle \sin^2(i) \rangle = 1.6$ for the dynamical mass (see e.g. Tacconi et al. 2008). For SMMJ163555 and SMMJ163541, we estimate the source size of 0.49 kpc and 0.89 kpc. This corresponds to the half-light radius, and to be able to compare with the results for other SMG results from Tacconi et al. (2008) we estimate the dynamical mass within $2R$ and find $M_{dyn} = 1.1 \times 10^{10}\ M_\odot$ and $1.0 \times 10^{10}\ M_\odot$, respectively. We note for SMMJ163555, that despite the large uncertainties in this estimate, this indicates that the molecular gas reservoir is a substantial fraction of the total mass for these galaxies. For SMMJ63541 we note that the molecular gas mass is higher than the estimated dynamical mass, and we assign this to a limited knowledge on

both X_{CO} and the dynamical state of the SMMJ163541 (e.g. the tentative second component would also contribute and could indicate that SMMJ163541 are interacting galaxies).

4.3. Star formation rate and efficiency

The star formation efficiency (SFE), i.e. how efficiently the molecular gas is being turned into stars, is often measured by the ratio L_{FIR}/M_{H_2}. We find an SFE of 440 $L_\odot/M_\odot$ for SMMJ163555 and 1000 $L_\odot/M_\odot$ for SMMJ163541, indicating that both these galaxies are forming stars more efficiently than the average local ULIRGs (e.g. Solomon et al. 1997). This is in good agreement with the previous SMG results from Neri et al. (2003) and Greve et al. (2005), who find a median value of 380 ± 170 $L_\odot/M_\odot$ and 450 ± 170 $L_\odot/M_\odot$, respectively.

For a Salpeter initial mass function with mass limits 0.1 and 100 $M_\odot$ we estimate the star formation rate (SFR) through $1.755 \times 10^{-10}\, L_{FIR}/L_\odot$ [$M_\odot\,yr^{-1}$] (Kennicutt 1998). For SMMJ163555 and SMMJ163541, we find an SFR of 80 $M_\odot\,yr^{-1}$ and 2600 $M_\odot\,yr^{-1}$. In rough numbers, the gas depletion time scale would be $\tau_{SMG} \sim 20$ Myr and ~8 Myr for SMMJ163555 and SMMJ163541 respectively, though these numbers would be higher if the dust is partly heated by a central AGN. The estimated time scales are somewhat below that from Greve et al. (2005) of $\tau_{SMG} \sim 40$ Myr, however, the individual estimates are likely to be affected by at least a factor two uncertainty arising from the assumptions about the IMF, the conversion between CO line luminosity to H_2 mass, and the far-infrared SED. In the case of SMMJ163555, which has a low far-infrared luminosity, it is likely that the CO-H_2 conversion factor is larger by a factor 2–3, implying a higher M_{gas} and therefore a time scale of 40–60 Myr. For SMMJ163541 we do not have a good constraint on the far-infrared SED and it is likely that the deduced SFR is overestimated, as demonstrated by Pope et al. (2006), who show that the 850 μm-determined SFR of SMGs is larger than that determined using 24 μm and radio observations. A lower SFR would imply a higher depletion time scale for SMMJ163541. Chapman et al. (2008) in a study of submm faint radio galaxies find a depletion time scale of ~11 Myr, which compared with the stellar mass, could suggest that those galaxies are seen towards the end of their current starburst episodes. Chapman et al. (2008) also discuss that these young ages could imply a very high duty cycle.

5. Conclusions

We have presented IRAM 3 mm spectroscopy for three SMGs in the field of A2218. CO detections were obtained for the sources SMMJ163555 at $z = 1.0313$ (CO(2–1)) and SMMJ163541 $z = 3.1824$ (CO(3–2)), confirming the optical redshifts. Both lines are shifted by −400 km s^{-1} relative to the optical redshift. The $z \approx 4$ candidate counterpart SMMJ163556 is undetected in CO(4–3) in the redshift range 4.035–4.082. Future observations at high angular resolution and other J-transitions are required for a more detailed study of the SMGs. Our results add to the still limited number of successful CO detections of SMGs.

When correcting for gravitational lensing, SMMJ163555 is so far the SMG known with the lowest far-infrared luminosity, and for the first time it allows us to probe the $L_{FIR} - L'_{CO}$ relation in the LIRG regime for high-redshift galaxies. Based on this one detection, we speculate that the high-redshift LIRGs have higher star formation efficiency than the nearby LIRGs. This can, however, only be clarified with a large sample using future sensitive instruments such as ALMA.

Acknowledgements. Based on observations carried out with the IRAM Plateau de Bure Interferometer. IRAM is supported by INSU/CNRS (France), MPG (Germany), and IGN (Spain). This work has benefited from research funding from the European Community's Sixth Framework Programme. J.P.K. thanks CNRS for support. This project was supported in part by the Deutsche Forschungsgemeinschaft (DFG) via grant SFB 494 and by the DFG Priority Programme 1177.

References

Baker, A. J., Tacconi, L. J., Genzel, R., Lehnert, M. D., & Lutz, D. 2004, ApJ, 604, 125
Barvainis, R., Tacconi, L., Antonucci, R., Alloin, D., & Coleman, P. 1994, Nature, 371, 586
Barvainis, R., Alloin, D., & Bremer, M. 2002, A&A, 385, 399
Biviano, A., Metcalfe, L., McBreen, B., et al. 2004, A&A, 425, 33
Blain, A. W., Smail, I., Ivison, R. J., Kneib, J.-P., & Frayer, D. T. 2002, Phys. Rep., 369, 111
Borys, C., Chapman, S., Donahue, M., et al. 2004, MNRAS, 352, 759
Bouché, N., Cresci, G., Davies, R., et al. 2007, ApJ, 671, 303
Chapman, S. C., Blain, A. W., Smail, I., & Ivison, R. J. 2005, ApJ, 622, 772
Chapman, S. C., Neri, R., Bertoldi, F., et al. 2008, ApJ, 689, 889
Coppin, K. E. K., Swinbank, A. M., Neri, R., et al. 2007, ApJ, 665, 936
Coppin, K. E. K., Swinbank, A. M., Neri, R., et al. 2008, MNRAS, 389, 45
Cox, P., Omont, A., Djorgovski, S. G., et al. 2002, A&A, 387, 406
Daddi, E., Dickinson, M., Chary, R., et al. 2005, ApJ, 631, L13
Daddi, E., Dannerbauer, H., Elbaz, D., et al. 2008, ApJ, 673, L21
Downes, D., & Solomon, P. M. 1998, ApJ, 507, 615
Downes, D., & Solomon, P. M. 2003, ApJ, 582, 37
Downes, D., Neri, R., Wiklind, T., Wilner, D. J., & Shaver, P. A. 1999, ApJ, 513, L1
Elíasdóttir, Á., Limousin, M., Richard, J., et al. 2008, ApJ, in press [arXiv:0710.5636]
Frayer, D. T., Ivison, R. J., Scoville, N. Z., et al. 1998, ApJ, 506, L7
Frayer, D. T., Ivison, R. J., Scoville, N. Z., et al. 1999, ApJ, 514, L13
Gao, Y., & Solomon, P. M. 2004, ApJS, 152, 63
Genzel, R., Baker, A. J., Tacconi, L. J., et al. 2003, ApJ, 584, 633
Greve, T. R., Bertoldi, F., Smail, I., et al. 2005, MNRAS, 359, 1165
Guilloteau, S., Omont, A., McMahon, R. G., Cox, P., & Petitjean, P. 1997, A&A, 328, L1
Guilloteau, S., Omont, A., Cox, P., McMahon, R. G., & Petitjean, P. 1999, A&A, 349, 363
Hainline, L. J., Scoville, N. Z., Yun, M. S., et al. 2004, ApJ, 609, 61
Kennicutt, Jr., R. C. 1998, ARA&A, 36, 189
Kneib, J. P., Mellier, Y., Fort, B., & Mathez, G. 1993, A&A, 273, 367
Kneib, J.-P., van der Werf, P. P., Kraiberg Knudsen, K., et al. 2004, MNRAS, 349, 1211
Kneib, J.-P., Neri, R., Smail, I., et al. 2005, A&A, 434, 819
Knudsen, K. K., van der Werf, P., Franx, M., et al. 2005, ApJ, 632, L9
Knudsen, K. K., Barnard, V. E., van der Werf, P. P., et al. 2006, MNRAS, 368, 487
Knudsen, K. K., Kneib, J.-P., & Egami, E. 2008a, in Infrared Diagnostics of Galaxy Evolution, ed. R.-R. Chary, H. I. Teplitz, & K. Sheth, ASP Conf. Ser., 381, 372
Knudsen, K. K., van der Werf, P. P., & Kneib, J.-P. 2008b, MNRAS, 384, 1611
Lapi, A., Shankar, F., Mao, J., et al. 2006, ApJ, 650, 42
Neri, R., Genzel, R., Ivison, R. J., et al. 2003, ApJ, 597, L113
Nesvadba, N. P. H., Lehnert, M. D., Genzel, R., et al. 2007, ApJ, 657, 725
Omont, A., Petitjean, P., Guilloteau, S., et al. 1996, Nature, 382, 428
Pelló, R., Le Borgne, J. F., Sanahuja, B., Mathez, G., & Fort, B. 1992, A&A, 266, 6
Planesas, P., Martin-Pintado, J., Neri, R., & Colina, L. 1999, Science, 286, 2493
Pope, A., Scott, D., Dickinson, M., et al. 2006, MNRAS, 370, 1185
Riechers, D. A., Walter, F., Carilli, C. L., et al. 2006, ApJ, 650, 604
Sanders, D. B., Scoville, N. Z., & Soifer, B. T. 1991, ApJ, 370, 158
Sheth, K., Blain, A. W., Kneib, J.-P., et al. 2004, ApJ, 614, L5
Smail, I., Ivison, R. J., Blain, A. W., & Kneib, J.-P. 2002, MNRAS, 331, 495
Solomon, P. M., Downes, D., Radford, S. J. E., & Barrett, J. W. 1997, ApJ, 478, 144
Tacconi, L. J., Neri, R., Chapman, S. C., et al. 2006, ApJ, 640, 228
Tacconi, L. J., Genzel, R., Smail, I., et al. 2008, ApJ, 680, 246
Walter, F., Bertoldi, F., Carilli, C., et al. 2003, Nature, 424, 406
Webb, T. M. A., Brodwin, M., Eales, S., & Lilly, S. J. 2004, ApJ, 605, 645
Weiß, A., Downes, D., Walter, F., & Henkel, C. 2005, A&A, 440, L45
Young, J. S., Schloerb, F. P., Kenney, J. D., & Lord, S. D. 1986, ApJ, 304, 443